INTERNATIONAL JOURNAL FOR NUMERICAL METHODS IN FLUIDS
Int. J. Numer. Meth. Fluids 2005; **47**:1269–1275
Published online 24 January 2005 in Wiley InterScience (www.interscience.wiley.com). DOI: 10.1002/fld.910

High order interpolation methods for semi-Lagrangian models of mobile-bed hydrodynamics on Cartesian grids with cut cells

Giorgio Rosatti[1,*,†], Roberto Chemotti[1] and Luca Bonaventura[1,2]

[1] *Dipartimento di Ingegneria Civile ed Ambientale, Mesiano di Povo 77, I-38050 (TN), Italy*
[2] *Max Planck Institut für Meteorologie, Bundesstr. 53, 20146 Hamburg, Germany*

SUMMARY

High order approximation methods based on radial basis functions are applied to the extension of semi-Lagrangian shallow water models to staggered Cartesian meshes with cut boundary cells. The accuracy and efficiency of the resulting semi-Lagrangian method is demonstrated by test cases simulating open channel flow. The derivative reconstruction provided by radial basis function interpolators is also employed successfully in the discretization of sediment transport models for mobile bed river flow. Copyright © 2005 John Wiley & Sons, Ltd.

KEY WORDS: radial basis functions; semi-Lagrangian method; cut cells; shallow water equations; mobile-bed flows

1. INTRODUCTION

A novel approach for modelling mobile-bed hydrodynamics is presented, obtained applying high order interpolation methods, using radial basis functions (RBF), to semi-implicit, semi-Lagrangian algorithms on staggered Cartesian meshes with cut boundary cells. A discretization with C-type staggering of the discrete variables is considered, as commonly employed in MAC-type discretizations [1] of two-dimensional fluid flow. It is assumed that the domain boundaries are described by segments of straight lines and that each boundary cell is intersected by at most a single straight line (Figure 1(a)). The choice of the cut cell approach is motivated by the fact that, with respect to standard rectangular cells, it allows to achieve an improved description of the boundaries while retaining the accuracy, efficiency and simplicity of the standard discretizations on Cartesian grid in absence of boundaries. It will be shown that accurate and efficient semi-Lagrangian methods are achieved, which allow to

*Correspondence to: Giorgio Rosatti, Dipartimento di Ingegneria Civile ed Ambientale, Mesiano di Povo 77, I-38050 (TN), Italy.
†E-mail: giorgio.rosatti@ing.unitn.it

Received 27 April 2004
Revised 5 October 2004
Accepted 5 October 2004

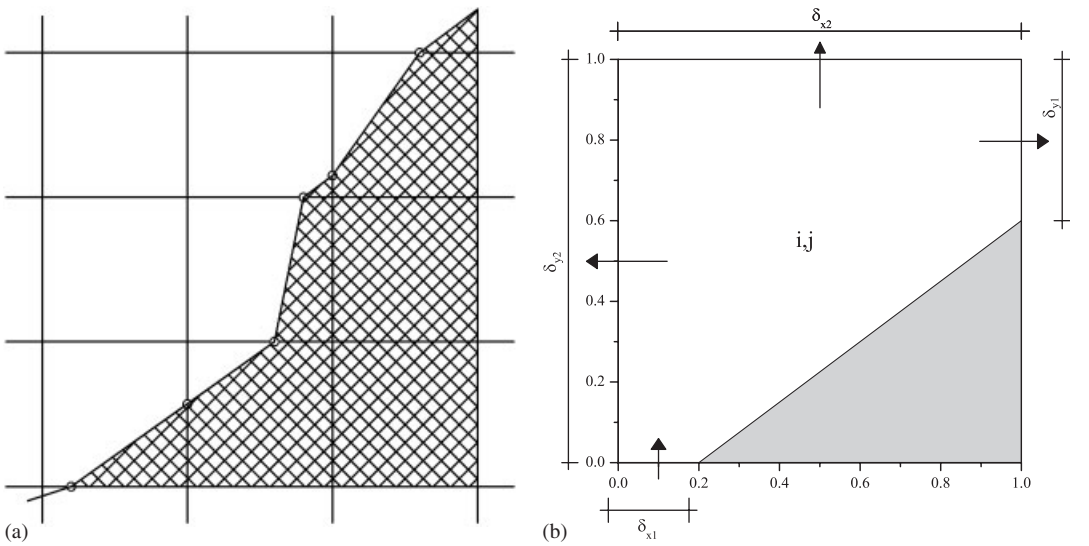

Figure 1. (a) Cut cells produced by piecewise linear approximation of the domain boundary; and (b) definition of the cut cell side fractions.

perform river flow simulations at high Courant numbers, thus allowing to reduce greatly the computational cost. This is very advantageous when performing long term simulations of mobile-bed hydrodynamics in rivers, estuaries and lagoons at low Froude numbers. Moreover, the high non-linearities that characterize sediment transport and morphological bed evolution require robust and accurate interpolation techniques along with an accurate description of the boundaries.

2. THE MODEL EQUATIONS AND THEIR CUT CELL DISCRETIZATION

The 2D hydrodynamical model consists of the depth-averaged water continuity and momentum equations

$$\begin{aligned} &\frac{\partial \eta}{\partial t} + \frac{\partial (UH)}{\partial x} + \frac{\partial (HV)}{\partial y} = 0 \\ &\frac{\partial U}{\partial t} + U\frac{\partial U}{\partial x} + V\frac{\partial U}{\partial y} = -g\frac{\partial \eta}{\partial x} - \frac{\tau_x^{\mathrm{b}}}{\rho H} \\ &\frac{\partial V}{\partial t} + U\frac{\partial V}{\partial x} + V\frac{\partial V}{\partial y} = -g\frac{\partial \eta}{\partial y} - \frac{\tau_y^{\mathrm{b}}}{\rho H} \end{aligned} \tag{1}$$

where g is the gravitational acceleration, U, V are the vertically averaged velocities in the x, y directions, respectively, η is the free surface elevation with respect to a reference horizontal plane, $H = \eta - z$ is the total fluid depth and z is the bottom surface elevation. τ_x^{b}, τ_y^{b} represent

the bed shear stresses and can be expressed as

$$\frac{\tau_x^{\mathrm{b}}}{\rho} = \gamma_{\mathrm{b}} U, \quad \frac{\tau_y^{\mathrm{b}}}{\rho} = \gamma_{\mathrm{b}} V \tag{2}$$

where ρ is the fluid density, $\gamma_{\mathrm{b}} = g\sqrt{U^2 + V^2}/\chi^2$ and χ is the Chézy coefficient for hydraulic roughness.

The mobile-bed model can be obtained adding the following sediment continuity equation to system (1):

$$\frac{\partial z}{\partial t} + \frac{\partial q_{sx}}{\partial x} + \frac{\partial q_{sy}}{\partial y} = 0 \tag{3}$$

in which q_{sx}, q_{sy} are the sediment transport rates per unit width in x and y directions, respectively. In the present model we assume uniform grain-size distribution and immediate adaptation of the sediment rate to the local depth-averaged flow parameters. The relation we used is the one proposed by van Rijn [2]

$$\frac{q_s}{\sqrt{g\Delta d}} = 0.053 \left[\frac{\theta - \theta_{\mathrm{cr}}}{\theta_{\mathrm{cr}}}\right]^{2.1} D_*^{-0.3} \tag{4}$$

where q_{b} is the module of the sediment transport rate per unit width, $\Delta = (\rho_s - \rho)/\rho$ is the relative density of the bed material respect water, d is the diameter of the sediment particles, $\theta = |\boldsymbol{\tau}|/(\gamma \Delta d)$ is the Shields parameter, θ_{cr} is the critical value of the Shields parameter and $D_* = d(g\Delta/\nu^2)^{1/3}$ is the characteristic adimensional sediment diameter. In subcritical flows, the sediment transport vector is not aligned with the depth-averaged velocity vector (for a detailed description of the problem see e.g. References [3, 4]): secondary flows in bends and gravity effects on sediment grains on a sloping bed generate a deviation of the direction of the sediment flow with respect to the depth-averaged water flow. In order to express these terms, an orthogonal, curvilinear co-ordinate system (s, n) is considered, where the s-axis is along the depth-averaged streamline, positive in the streamwise direction, and n is the principal unit normal vector. Secondary flow generates a bottom stress in n direction that can be expressed (see e.g. Reference [5]) as

$$\tau_n = \rho \alpha |\mathbf{U}|^2 \frac{H}{R}; \quad \frac{1}{R} = -\frac{UV((\partial V/\partial y) - (\partial U/\partial x))}{(\sqrt{U^2 + V^2})^3} \tag{5}$$

where α has a value in the range between 0.02 and 0.06, $|\mathbf{U}|$ is the depth-averaged velocity module, H is the water depth and R is the streamline curvature radius. The value of $|\boldsymbol{\tau}|$, to be used in (4), is given by $|\boldsymbol{\tau}| = \sqrt{\tau_s^2 + \tau_n^2}$, where τ_s is obtained from the solution of the hydrodynamical model. Gravity rotates the sediment transport rate vector $\mathbf{q}_{\mathrm{b}}$ in such a way that the component of the vector along the s and n directions, following Reference [6], becomes

$$q_s = \frac{q_{\mathrm{b}}}{\sqrt{1 + \left(\dfrac{r}{\sqrt{\theta}} \dfrac{\partial z}{\partial n}\right)^2}}; \quad q_n = r \frac{q_s}{\sqrt{\theta}} \frac{\partial z}{\partial n} \tag{6}$$

where r is a parameter whose value is in the range between 0.3 and 0.6 and $\partial z/\partial n$ is the slope of the bottom in the normal direction. The value of q_{sx}, q_{sy}, to be used in (3), can be easily obtained projecting q_s and q_n along the x- and y-axis.

Table I. Accuracy of RBF interpolators (MQ = multiquad., TPS = thin plate spl.) for the x component of the velocity on a Cartesian grid with cut cells.

	l_∞ error		l_2 error		Conv. rate in l_∞		Conv. rate in l_2	
$\varepsilon\Delta x$	MQ	TPS	MQ	TPS	MQ	TPS	MQ	TPS
1/6	3.8×10^{-2}	5.7×10^{-2}	2.2×10^{-6}	2.3×10^{-5}	—	—	—	—
1/12	1.1×10^{-2}	1.5×10^{-2}	3.1×10^{-6}	4.5×10^{-6}	1.8	1.9	2.8	2.4
1/24	2.8×10^{-3}	5.3×10^{-3}	2.9×10^{-7}	9.1×10^{-7}	1.9	1.5	3.4	2.3
1/48	1.0×10^{-3}	2.0×10^{-3}	3.6×10^{-8}	2.0×10^{-7}	1.5	1.4	3.0	2.1

We consider now the introduction of an improved description of the boundaries in the context of a Cartesian grid approach. We assume that the domain boundaries are described by segments of straight lines and that each boundary cell is intersected by at most a single straight line (see Figure 1(a)). As stated above, even if this is *a priori* limitation, it allows to rule out the too complicated subgrid behaviour of the boundaries. Anyhow it is sufficiently general to allow for appropriate boundary description in most environmental flows. Let $\delta_{i+1/2,j}, \delta_{i,j+1/2}$ denote the lengths of the cut cell sides fractions that are within the computational domain in the x, y directions, respectively (see Figure 1(b)). Denote the area of the cut cell (i,j) by $A_{i,j}$ and let $\Theta_{i,j} = A_{i,j}/(\Delta x \Delta y)$.

The finite difference, semi-implicit discretization of the shallow water equations introduced in Reference [7] and used successfully in a number of practical applications (see e.g. Reference [8]) is extended by introducing the quantities $\delta_{i+1/2,j}, \delta_{i,j+1/2}$ and $\Theta_{i,j}$ in the computation of the mass and sediment fluxes. Furthermore, velocity component locations along the cut cell edges are moved to the midpoint of the part of the edge that belongs to the computational domain.

In the semi-Lagrangian method and in the computation of the sediment fluxes, radial basis function (RBF) interpolations are used to obtain the values of the velocity components in points of the grids where they are not defined (e.g. the V component in position $i+1\ 2, j$) as well as derivatives of the variables that are necessary to compute (4). RBF are an interpolation technique for scattered multivariate data that has been studied in depth over the last two decades (see e.g. the review in Reference [9]). When appropriate radial basis functions are chosen, spectral convergence rates can be achieved (see e.g. References [10, 11]). It can also be shown that the derivatives of the interpolated function can be approximated just as accurately by the derivative of the RBF interpolator. To the best of our knowledge, RBF interpolators have been used in high order finite volume methods, but not in conjunction with cut cell approaches. The effective accuracy and robustness for the reconstruction of scalar and vector fields on Cartesian grids with cut cells will now be demonstrated by a simple example. In this test, a stencil of $N = 10$ points was used and the RBF interpolator was constrained to fit linear polynomials in x, y exactly (see e.g. Reference [9]). The basis functions used were the multiquadric (MQ) and the thin plate spline (TPS) $\phi(x) = (\varepsilon x)^2 \log \varepsilon x$. Results obtained with other basis functions such as the Gaussian $\phi(x) = e^{-(\varepsilon x)^2}$ or the Inverse-Multiquadric $\phi(x) = 1/\sqrt{1+(x\varepsilon)^2}$ were entirely analogous to those obtained with MQ. The function to be interpolated was taken to be the U component of an analytic velocity field representing 2D potential flow around an infinite cylinder with far field velocity U_0 aligned with the x-axis. The error behaviour is shown in Table I.

3. NUMERICAL TESTS

Numerical tests of the previously described approach were performed first with a two-dimensional model of shallow water flow over a fixed bed. As a first test, uniform flow in a straight open channel with rectangular section was considered, for which an analytic solution is available. In order to check the accuracy of the proposed cut cell approach, the channel was oriented at $\alpha = 22.8°$ with respect to a rectangular Cartesian mesh. Simulations were performed using Courant numbers with respect to the velocity equal to 3.23 and 1.28 in x and y directions, respectively. The resulting relative errors of the velocity components and of the water depth with respect to the analytical solution were of the order 10^{-4} and 10^{-8} in the l_∞ and l_2 norm, respectively. Similar values can be obtained with a standard discretization on a Cartesian grid if a channel aligned with the grid is considered.

Another test was run with analogous boundary conditions in the case of a curved channel. The channel had rectangular section 2.5 m wide, slope $i_b = 0.35 \times 10^{-3}$ and the Chézy coefficient was taken to be equal to 83.4 $m^{1/2}/s$. Two orthogonal straight reaches were connected with a curved one, bounded by two quarters of circle with radii 12.5 and 15 m, respectively. A rectangular Cartesian mesh with $\Delta x = \Delta y$ equal to 0.1 m was used. Simulations were performed using a timestep equal to 0.9 s and therefore the Courant number (with respect to the velocity) was approximately equal to 4.8. The computed value for the deviation of the free surface from the horizontal along the cross section at 45° of the curved part of the channel is 0.0052 m, which agrees very well with analytical estimates of 5.2062×10^{-3} m (see e.g. Reference [12]).

In order to test the model in a case with sediment transport and mobile bed, the same setup was considered as in the curved channel fixed bed case. At the upstream boundary, the water discharge was the same as in the previous test while the sediment discharge was $q_s = 1.58 \times 10^{-7}$ m^3/s. Results of the bottom configuration after 130 h of simulations are compared with a laboratory experiment, from Reference [13], similar to the numerical one, see Figure 2. The lack of description of boundary conditions for the experimental test did not allow to reproduce exactly that test, so the comparison is only qualitative.

It is possible to notice that all the main features of the bottom topography are well captured by the numerical model. At the entrance of the curve, deposition is at the outer side of the

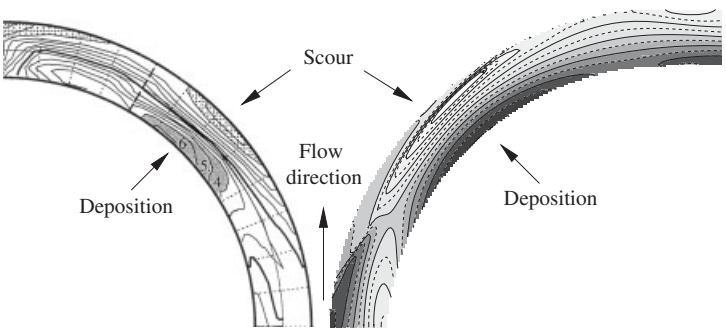

Figure 2. Comparison between asymptotic bottom elevations obtained, on the left, with laboratory data (from Reference [13]), and on the right, with the present numerical model.

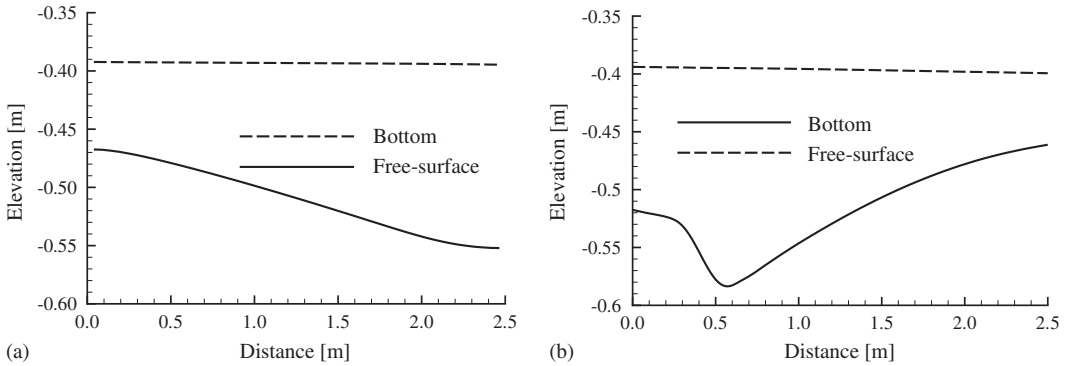

Figure 3. Cross sections of the bottom configurations obtained with the numerical model after 130 h of simulations: (a) at the entrance of the curve; and (b) at a radial section at 45°.

channel and scour is near the inner side. Downstream, the situation is the opposite and a point bar is obtained at the inner side of the curve while the scour is located at the outer side. In the curved reach, maximum scour and deposition are obtained in a section at 45°, while another maximum/minimum is localized at the end of the curve.

A more quantitative estimate of the quality of the numerical results can be obtained comparing the slope of the bottom in the section at 45° obtained with the numerical model with the semi-empirical expression proposed in Reference [3]: $S_n = Cd/r$ where S_n is the bottom slope in the normal direction $C \simeq 7 \tan(\pi/6)$, H is the local water depth and r is the mean curvature radius of the channel. The numerical model gives a value of the bottom slope equal to 5.35×10^{-2} while the semi-empirical estimate, evaluated with average values of water depth and curvature radius, respectively, $H = 0.11$ m and $r = 13.75$ m, gives a value equal to 3.31×10^{-2}. This result is significant because the semi-empirical relation is a rather crude estimate and only gives the correct order of magnitude for the slope. Finally, it can be noticed that the bottom profile is smooth also near the boundaries, see Figure 3. Since small perturbations are strongly amplified by the high non-linearity of the sediment transport relations, they can generate relevant bottom variations; the lack of these features in the numerical results is an indirect confirmation of the lack of spurious effects at the boundaries.

REFERENCES

1. Harlow FH, Welch JE. Numerical calculation of time dependent viscous incompressible flow. *Physics of Fluids* 1965; **8**:2182–2189.
2. van Rijn LC. Sediment transport, part I: bed load transport. *Journal of Hydraulic Engineering* 1984; **110**: 1613–1641.
3. Odgaard AJ, Bergs MA. Flow processes in curved alluvial channel. *Water Resource Research* 1988; **24**:45–56.
4. Parker G, Andrews ED. Sorting of bed load sediment by flow in meander bends. *Water Resource Research* 1985; **21**:1361–1373.
5. Zimmermann C, Kennedy JF. Transverse bed slopes in curved alluvial streams. *ASCE Journal of Hydraulic Division* 1978; **104**:33–48.
6. Ikeda S. Lateral bed load transport on side slopes. *Journal of Hydraulic Division* 1983; **108**:1369–1373.
7. Casulli V. Semi-implicit finite difference methods for the two dimensional shallow water equations. *Journal of Computational Physics* 1990; **86**:56–74.

8. Gross ES, Koseff JR, Monismith SG. Three-dimensional salinity simulations of South San Francisco Bay, *ASCE Journal of Hydraulic Engineering* 1999; **125**:1199–1209.
9. Buhmann MD. Radial basis functions: the state-of-the-art and new results. *Acta Numerica* 2000; **9**:1–37.
10. Li X, Micchelli CA. Approximation by radial bases and neural networks. *Numerical Algorithms* 2000; **25**: 242–262.
11. Schaback R, Wu Z. Local error estimates for radial basis function interpolation of scattered data. *IMA Journal of Numerical Analysis* 1993; **13**:13–27.
12. Henderson FM. *Open Channel Flow*. McMillan: New York, 1966.
13. Blanckaert K, Graf WH. Mean flow and turbulence in open-channel bend. *Journal of Hydraulic Engineering* 2001; **10**:835–847.

